communications physics

A Nature Portfolio journal

Article

https://doi.org/10.1038/s42005-025-02070-9

Testing Adam-Gibbs relationship in tapped granular packings

Xinyu Ai [1], Houfei Yuan [2], Shuyang Zhang [2], Zhikun Zeng [2], Hanyu Li[1], Chengjie Xia [3] ✉ & Yujie Wang [1,2,4] ✉

Disordered granular packings share many similarities with supercooled liquids, particularly in the rapid increase of structural relaxation time within a narrow range of temperature or packing fraction. However, it is unclear whether the dynamics of granular materials align with those of their corresponding thermal hard sphere liquids, and the specific influence of friction in a granular system remains largely unexplored. Here, we experimentally study the slow relaxation and the steady state of monodisperse granular sphere packings under vertical tapping using X-ray tomography. We first calculate the thermodynamic parameters including the effective temperature and configurational entropy under the Edwards' ensemble of packings of granular spheres with varying friction, and measure their characteristic relaxation time during compaction. We then present a unified picture of the relaxation process in granular systems, in which a generalized Adam-Gibbs relationship is followed. These results clarify the close relationship between granular materials and the ideal frictionless hard sphere model.

Granular matter is ubiquitous in nature and daily life. Due to dissipative interactions among granular particles and the negligible thermal agitation energy compared to the gravitational potential energy[1], granular materials ordinarily remain in stable packing states without external energy injection. Consequently, a granular packing is often regarded as being at "zero temperature" and lacking the ergodicity of exploring the phase space as a thermal system, hence making it difficult to study using traditional equilibrium theories. On the other hand, the packing structure of granular spheres has been considered to be close to that of atomic liquids and glasses[2,3], and granular materials are often regarded as macroscopic models of glass-forming systems[4]. Also, the slow relaxation dynamics and dynamic heterogeneity behaviors of granular materials under external perturbation bear a close resemblance to those of glass-forming materials[5–7]. For example, the compaction processes of granular packings can be qualitatively fitted using similar slow dynamics laws obeyed by glassy systems[8,9], suggesting that the structural relaxation mechanism of glass systems could, in principle, be applied to macroscopic and frictional granular materials. The glassy dynamics represents one of the most challenging problems in condensed matter physics, and the thermodynamic origin of the slow dynamics in granular matter remains unresolved. Particularly, a quantitative correspondence between granular systems with different friction coefficients and a frictionless hard sphere liquid has not yet been truly developed.

We think examining the effective thermodynamic nature underlying the relaxation dynamics of granular packings would help establish a convincing mapping between the granular and glass systems. Among the many theories explaining the origin of slow dynamics of glassy materials, the Adam-Gibbs (AG) relation is the first to highlight a possible thermodynamic origin[10]. By introducing the notion of cooperative rearranging regions (CRRs), which are the smallest regions where rearrangement can take place independently, the AG relation establishes a direct link between configurational entropy and relaxation time, and thus underscores the vital role of thermodynamics in glass transition. Over the past 30 years, a considerable number of simulations and experiments have validated the AG relation in various supercooled liquids[11–16]. The physical implications of the AG relationship and CRRs remained elusive until the development of the Random First Order Transition (RFOT) theory by Wolynes, Kirkpatrick, and Thirumalai in the 1980s[17]. Within RFOT, the change in free energy during the rearrangement of CRRs (i.e., mosaics) consists of a surface term representing the increase (cost) in free energy due to the mismatch at the interfaces of different mosaics, and a bulk term reflecting the decrease (gain)

[1]School of Physics, Chengdu University of Technology, Chengdu, 610059, China. [2]School of Physics and Astronomy, Shanghai Jiao Tong University, Shanghai, 200240, China. [3]Shanghai Key Laboratory of Magnetic Resonance, School of Physics and Electronic Science, East China Normal University, Shanghai, 200241, China. [4]State Key Laboratory of Geohazard Prevention and Geoenvironment Protection, Chengdu University of Technology, Chengdu, 610059, China.
✉e-mail: cjxia@phy.ecnu.edu.cn; yujiewang@sjtu.edu.cn

in free energy driven by the change in entropy of the CRR as rearrangements occur[18]. The change in free energy when CRRs grow can be expressed as:

$$\Delta F = \gamma\xi^{\theta} - TS_c\xi^{d}, \tag{1}$$

where γ is the surface tension, θ is the surface dimension, d is the spatial dimension, T is temperature, S_c is the configurational entropy density, and ξ is the linear size of the mosaics. The typical mosaic size,

$$\xi \propto \left(\frac{1}{TS_c}\right)^{\frac{1}{d-\theta}}, \tag{2}$$

can be obtained by setting $\Delta F = 0$. In addition, the relaxation process in a supercooled liquid is considered as a thermal activation[19,20], leading to a relationship between structural relaxation time τ and the energy barrier, which is assumed to be proportional to ξ^{ψ},

$$log\left(\frac{\tau}{\tau_0}\right) \propto \frac{\xi^{\psi}}{T}. \tag{3}$$

Combining (2) and (3), we obtain the relation:

$$log\left(\frac{\tau}{\tau_0}\right) \propto \left(\frac{1}{TS_c}\right)^{\frac{\psi}{d-\theta}}. \tag{4}$$

Within RFOT, Kirkpatrick and Wolynes propose that the exponents $\theta = \psi = d/2$[17], and therefore recover the original AG relation.

Given the success of the AG relation in glassy liquid systems, the question of whether it is still valid in disordered granular materials remains unresolved. The distinctive characteristic of granular packings is their static nature, hence kinetic entropy is inherently absent, making the calculation of configurational entropy more straightforward compared to the challenges of distinguishing configurational entropy from the kinetic one in a supercooled liquid. In addition, during a typical experimental procedure for preparing a granular packing[21], the system is reasonably supercooled, where the AG relation is believed to be applicable. In fact, our recent study has tested the AG relation in granular material systems based on the entropy obtained within the Edwards volume ensemble[22]. However, a rigorous relationship between the Edwards entropy and the original configurational entropy of a corresponding hard sphere liquid has not been established. This is particularly unclear since the Edwards entropy depends on friction, a unique property of mechanically stable granular packings, which is irrelevant for a supercooled hard sphere liquid. It therefore remains a fundamental open question whether frictional granular systems share the same thermodynamic origin of slow relaxation as their frictionless thermal counterpart.

In this study, we investigate the structure and the corresponding structural relaxation time of tapped granular packings using X-ray tomography. By calculating the configurational entropy based on the Edwards volume ensemble, we test the applicability of AG relation for four types of

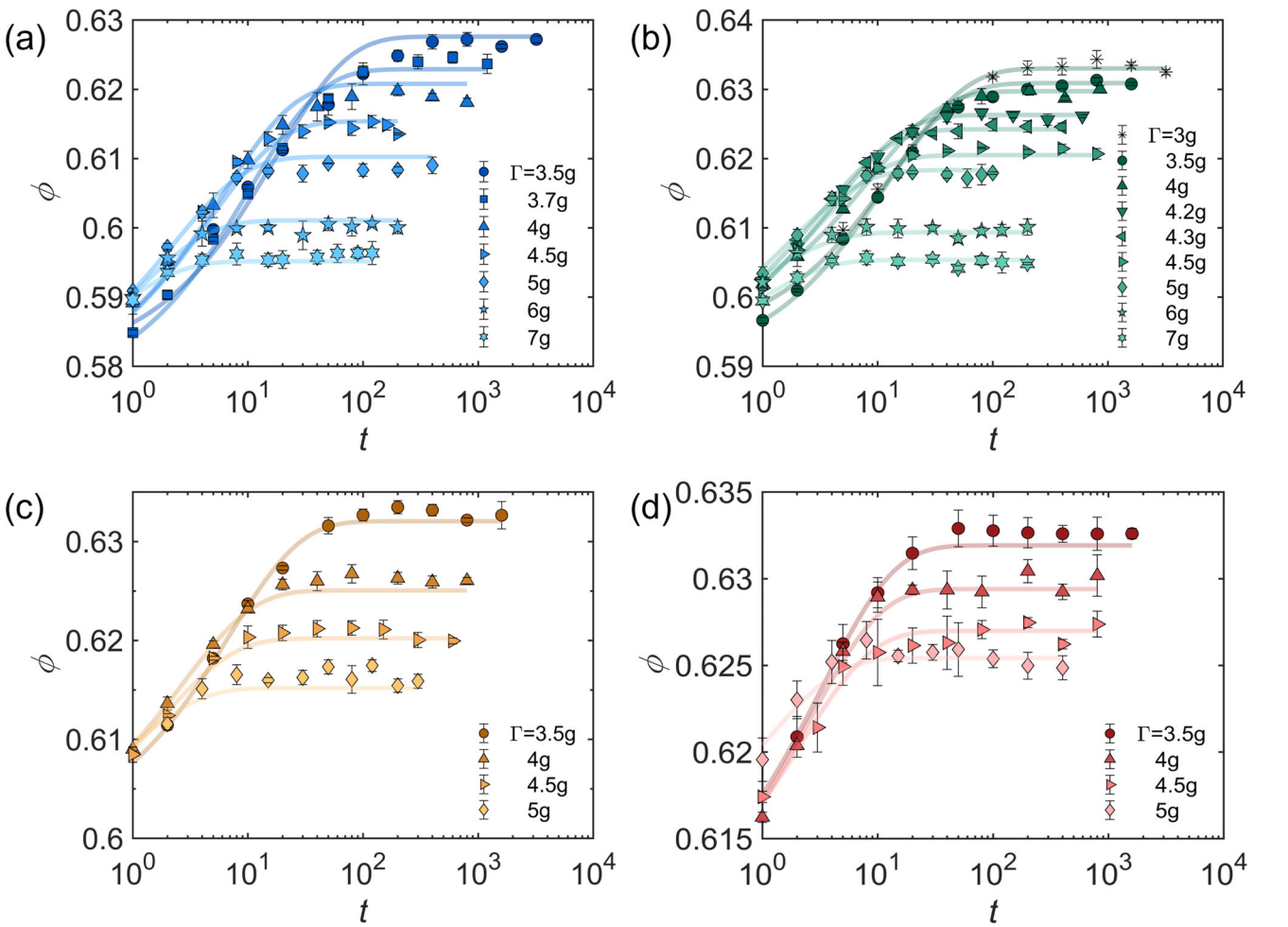

Fig. 1 | Compaction curves of tapped granular packings. Packing fraction ϕ as a function of tap number t with different tap intensities Γ, for the four types of granular spheres: **a** BUMP, **b** 3DP, **c** ABS2, and **d** ABS1. Solid curves represent the Kohlrausch–Williams–Watts (KWW) function fitting results according to Eq. (5). Each data point represents the average of three independently repeated experiments, and the error bars represent the standard deviations. The definition of error bars is consistent across all subsequent figures.

Table 1 | KWW fitting results

Systems	$\langle\phi_\infty\rangle$	$\langle\phi_\infty\rangle - \langle\phi_0\rangle$	$\langle\tau\rangle$
BUMP	0.6276	0.0473	17.56
	0.6229	0.0471	10.39
	0.6208	0.0435	6.07
	0.6154	0.0391	4.57
	0.6103	0.0340	2.28
	0.6011	0.0267	1.13
	0.5952	0.0201	0.63
3DP	0.6330	0.0397	14.31
	0.6309	0.0411	11.43
	0.6297	0.0343	8.64
	0.6263	0.0354	4.11
	0.6242	0.0330	3.17
	0.6205	0.0313	2.60
	0.6183	0.0277	1.77
	0.6094	0.0168	1.04
	0.6054	0.0178	0.80
ABS2	0.6321	0.0317	6.84
	0.6251	0.0257	2.70
	0.6202	0.0214	1.84
	0.6152	0.0162	0.95
ABS1	0.6319	0.0221	3.34
	0.6294	0.0207	2.55
	0.6270	0.0178	2.14
	0.6254	0.0128	1.10

$\langle\phi_\infty\rangle$ is the average steady state packing fraction of five independent measurements. In the fitting of each compaction curve, $\phi_\infty - \phi_0$ and τ are set as free parameters, and the averaged values obtained from three independent compact curves are shown in the table.
KWW Kohlrausch–Williams–Watts.

granular spheres with different friction coefficients (i.e., roughness). We find that the AG relation is clearly observed in our systems over the reasonably long timescale for the structural relaxation time, once the influence of friction is removed through proper rescaling of the Edwards entropy. This suggests that the underlying assumption of the AG relation that configurational entropy plays a pivotal role in the occurrence of slow dynamics is also valid for granular systems.

Results

In order to obtain the dynamical and structural variables of granular packings, we prepare packings consisting of four types of monodisperse beads with varying friction coefficients. We tap the packings at different tap intensities using an electric shaker, and record the packing structures after various numbers of taps by CT scans. Packings are initially prepared in a loose state with 10 taps at an intensity of $\Gamma = 12g$, where g is the gravitational acceleration constant. After a large number of taps, the packing fraction eventually reaches a constant value, representing a steady state. Packing structures at different steady states under varying tap intensities are recorded with X-ray tomography and analyzed. Each packing consists of 6000 to 8000 spheres with a diameter D of about 6 mm, and is prepared in a cylindrical container with an inner diameter of $22.5D$. Detailed descriptions of the granular samples and experimental methods can be found in the methods section.

Compaction and slow relaxation

To study the slow relaxation process under different tap intensities, we fit the evolution of the packing fraction as a function of the tap times, i.e., the compaction curves, using the Kohlrausch–Williams–Watts (KWW) form (Fig. 1a–d):

$$\phi(t) = \phi_\infty - (\phi_\infty - \phi_0)exp\left[-(t/\tau)^\beta\right], \tag{5}$$

from which we obtain the characteristic relaxation time τ of the system. Here, ϕ_∞ and ϕ_0 represent the steady-state and the initial packing fraction, respectively, with ϕ_∞ values determined from five independent measurements of the steady-state packing fractions (as shown in Table 1). In the fitting, we fix the value of β at 0.7 to reduce the number of free parameters and improve the reliability of the fitting. We have also validated that the obtained values of τ remained essentially unchanged even when all parameters were allowed to vary during fitting, with β fluctuating around 0.7 and show no dependence on tap intensity or bead type. The fitting results are presented in Table 1.

As shown in Fig. 2a, the steady-state packing fraction decreases with increasing tap intensity Γ, consistent with previous results[23–25]. According to our recent study on Edwards volume ensemble[26], a larger Γ corresponds to a higher effective temperature and higher weight of exploring loose packing states, resulting in a lower ensemble-averaged packing fraction. Moreover, the range of accessible packing fraction increases with particle friction coefficient, which can be attributed to the enhanced density of mechanically stable states[26].

Edwards volume ensemble

We further obtain the thermodynamic variables of the packings by analyzing the stationary state packing structures based on the Edwards volume ensemble theory, a generalized statistical mechanical framework developed for granular systems. This theory has been widely used and validated in various granular packings, regarding statistical mechanical and thermodynamic principles such as the Boltzmann distribution, the zeroth law, and the fluctuation-dissipation theorem[26,27].

According to the Edwards volume ensemble, the compactivity χ, which serves as the effective temperature, can be calculated using an analogous fluctuation theorem:

$$\frac{1}{\chi(\phi)} = \int_{\phi_{RLP}}^{\phi} \frac{d\varphi}{\varphi^2 var(V)}, \tag{6}$$

where $var(V) = \sigma^2(V)/m$, $\sigma^2(V)$ is the variance of reduced volume of coarse-grained Voronoi cells, with $V = \sum_m V_{voro}/mV_p$ and $m = 15$ is the number of particles within the coarse-grain spherical region (i.e., a region containing the nearest m neighbors of each central particle). ϕ_{RLP} is the packing fraction of the random loose packing (RLP), with values of 0.568, 0.587, 0.593, and 0.605 for the four types of spheres with different roughness. We use a cubic polynomial to fit the volume variance as a function of ϕ: $var(V) = 0.3810 - 0.5908\phi - 0.5214\phi^2 + 0.8392\phi^3$ (see Fig. 2b), and then perform a numerical integration to obtain χ, whose relationship with the packing fraction is shown in Fig. 2c. The configurational entropy S_c, representing the logarithm of the number of mechanical stable packing states, can be calculated from another thermodynamic relation:

$$S_c(\phi) - S_{RCP} = \int_{\phi}^{\phi_{RCP}} \frac{d\varphi}{\varphi^2 \chi(\varphi)}, \tag{7}$$

as shown in Fig. 2d. Here, ϕ_{RCP} is packing fraction of the random close packing (RCP), and the entropy S_{RCP} of RCP is set to 1.1 as the Shannon entropy estimated by Briscoe et al.[28]. More detailed discussion regarding the calculation of these thermodynamic quantities can be found in our previous work[26].

As shown in Fig. 2c, d, these thermodynamic equations of the state vary with friction. Consistently, the compactivity decreases with increasing packing fraction, ranging from infinity at RLP to nearly zero around RCP. The configurational entropy also decreases with ϕ, similar to that of a hard

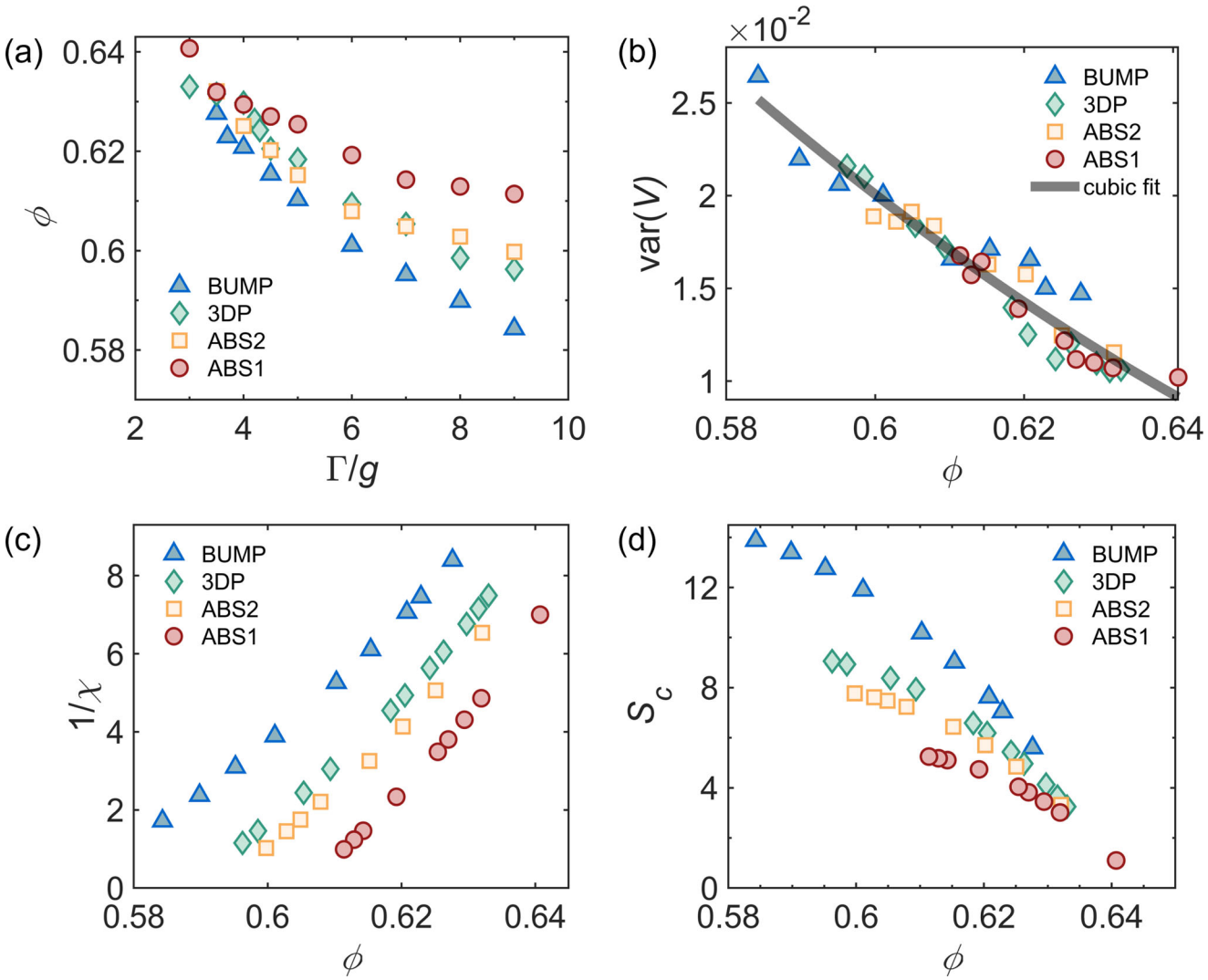

Fig. 2 | Thermodynamics of various frictional systems. a The steady state packing fraction ϕ as a function of tap intensity Γ, for BUMP (blue Deltas), 3DP (green diamonds), ABS2 (yellow squares), and ABS1 (red circles) systems. **b** Coarse-grained Voronoi volume variance var(V) as a function of ϕ. The solid curve is a cubic polynomial fit. **c** Inversed compactivity $1/\chi$ as a function of ϕ. **d** Configurational entropy S_c as a function of ϕ.

sphere glass. S_c is larger for rougher particles because more configurations can maintain mechanical stability at the same packing fraction.

Thermodynamic origin of relaxation dynamics

We now examine the relationships between relaxation time τ and thermodynamic quantities: compactivity χ and configurational entropy S_c. As shown in Fig. 3a, τ increases rapidly as χ decreases, which can be well described by the Vogel–Fulcher–Tamman (VFT) form for glassy systems. It is worth noting that the $\tau \sim \chi$ relationships for the four types of spheres with different friction coefficients are on the same curve in contrast to the friction-dependent behaviors of $\tau \sim \phi$. This direct collapse of $\tau \sim \chi$ relationships indicates that the frictional effects on the relaxation dynamics of tapped granular packings are negligible and could be entirely removed when establishing the thermodynamic-dynamic relationships. This suggests a universal dependence of the structural relaxation time on compactivity or tap intensity instead of packing fraction, as we have verified that different systems possess identical compactivity under the same Γ with previous experiments[26]. This behavior is likely due to the fact that, during the tapping process, the system relaxes mainly during the heated phase, corresponding to liquid-like configurations when particles are colliding without frictional contacts. The effects of friction come into play only when the system is rapidly quenched to the jammed state, at which the system is frozen and can no longer relax[29].

In contrast with the $\tau \sim \chi$ relationship, the relationships between relaxation time and Edwards entropy are friction-dependent (Fig. 3c). We note that the Edwards entropy is not equivalent to the configurational entropy of a hard sphere liquid, as the number of mechanically stable states within each basin of the landscape depends on friction. These states do not have a one-to-one correspondence with the liquid configurations when structural relaxation occurs. Therefore, we need to use the configurational entropy associated with the liquid state to test the AG relation. Consistent with our previous study[29], we can linearly rescale the configurational entropy and packing fraction of different systems by defining $\widetilde{S} = \frac{S_c - S_{RCP}}{S_{RLP} - S_{RCP}} + \widetilde{S}_{RCP}$ (where S_{RLP} is the Edwards entropy of RLP), and $\widetilde{\phi} = \frac{\phi - \phi_{RLP}}{\phi_{RCP} - \phi_{RLP}}$. After this rescaling, the $\widetilde{S} \sim \widetilde{\phi}$ relationships collapse across different systems (Fig. 3b). The friction-independence of the rescaled configuration entropy $\widetilde{S}$ suggests that it is associated with the corresponding liquid state when the granular packing is agitated during the tapping processes, and could be the true thermodynamic origin of the dynamic relaxation.

In this rescaling, the rescaled configurational entropy of RCP is shifted from 0 to 0.5 by the additional $\widetilde{S}_{RCP}$, and accordingly, the

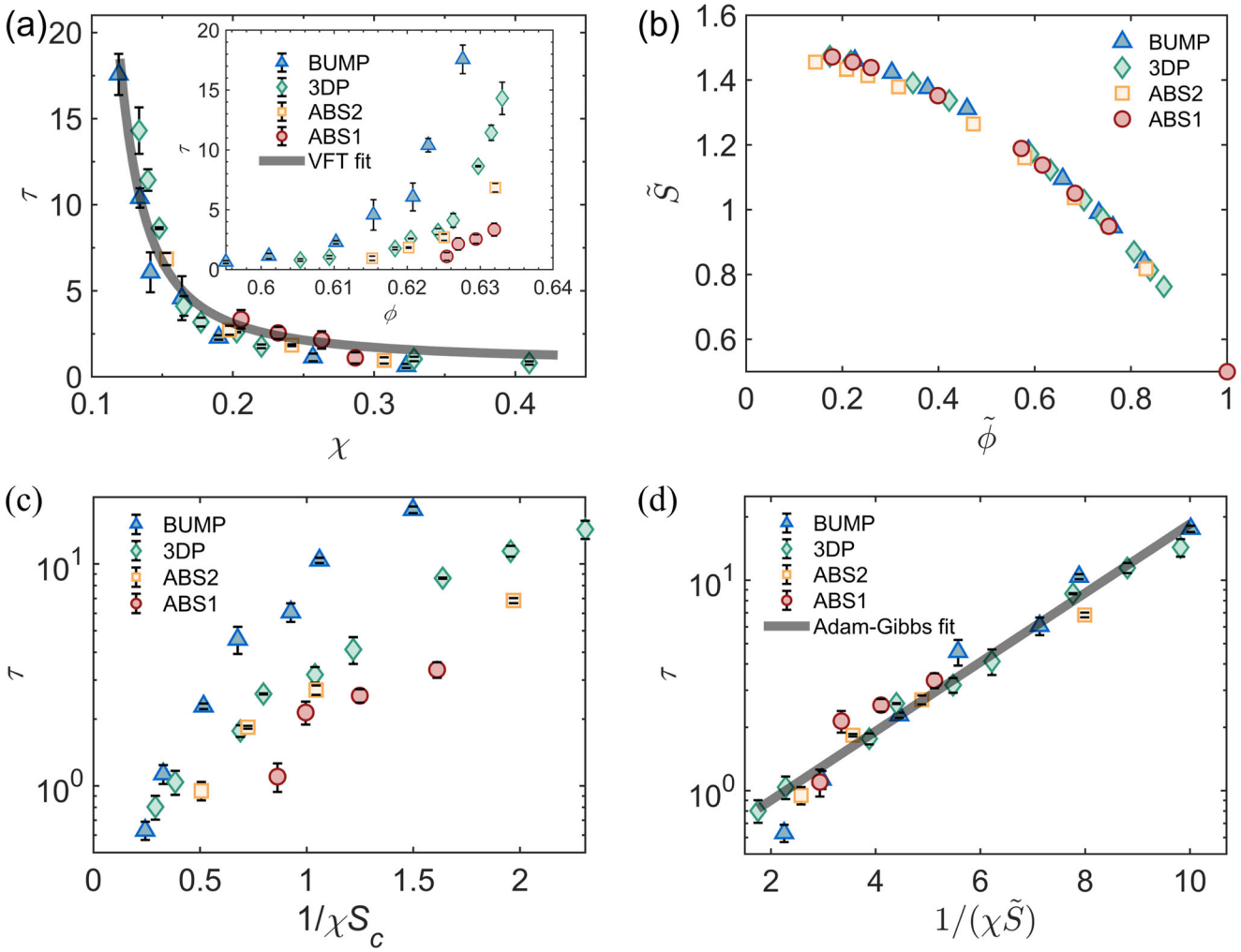

Fig. 3 | Relationships between dynamical and thermodynamical variables. **a** Relaxation time τ versus χ for BUMP (blue Deltas), 3DP (green diamonds), ABS2 (yellow squares), and ABS1 (red circles) systems. The solid curve is a fit of the VFT form: $\tau = \tau_0 \exp\left[D\chi_0/(\chi - \chi_0)\right]$. Inset: τ as a function of ϕ. **b** Rescaled configurational entropy $\widetilde{S}$ versus rescaled packing fraction $\widetilde{\phi}$. **c** Relaxation time τ versus $1/\chi S_c$ for the four systems. **d** Relaxation time τ versus $1/\chi\widetilde{S}$. The solid curve is a fit of the Adam-Gibbs relationship: $\tau \sim \exp[A/\chi\widetilde{S}]$, where A is a constant. VFT Vogel–Fulcher–Tammann.

rescaled configurational entropy for RLP becomes $\widetilde{S}_{RLP} = 1.5$. By doing this, the behavior of rescaled entropy $\widetilde{S}$ closely resembles that of a frictionless hard sphere liquid between the onset temperature T_{onset} and the dynamical glass transition temperature T_d. This is consistent with the interpretation that RLP and RCP correspond to a hard sphere glass at T_{onset} and T_d, respectively[29]. The two bounds of the rescaled entropy represent the dimensionless configurational entropy per particle at T_{onset} and T_d according to a previous numerical simulation[30]. This small range of the corresponding temperatures also explains why the one-decade increasing in the relaxation timescale obtained in this work and other similar granular systems is significantly smaller than that of a typical molecular liquid during the glass transition[31,32].

Based on this rescaled entropy, we plot τ as a function of $\chi\widetilde{S}$ in accordance with the AG relationship in Fig. 3d. Surprisingly, again all the curves collapse onto the same master curve. This in turn suggests that the structural relaxation time is predominantly controlled by the configurational entropy associated with the corresponding liquid state, rather than by the frictional ones. The master curve closely matches the predictions of the AG theory, which appears as a straight line on the semi-logarithmic plot, confirming that the original AG relationship is recovered.

Discussion

At last, we discuss whether and how the physical picture of the RFOT theory matches with the structural relaxation of our granular systems. According to Eq. (4), there exist many potentially valid combinations of values of ψ and θ that can give the correct AG relation. The RFOT theory predicts that $\theta = \psi = d/2$[17]. Yet, recent experiments indicate that θ is slightly greater than 2, leading to a ψ value lower than that predicted by RFOT[22,33]. Since ψ is related to the potential barrier between the initial and final configurations, this relatively small ψ indicates that the energy barrier does not grow as rapidly as the size of the CRR if activation is the only mechanism for structural relaxation, and some other dynamic relaxation mechanisms may also be working in this regime as discussed below.

It should be noted that the granular packing corresponds to a hard sphere liquid quenched between T_{onset} and T_d. In this temperature range, where the system is not deeply supercooled, the AG relationship is not expected to hold rigorously, as the activation-dominated regime should typically lie below the dynamical transition temperature T_d. However, some studies have pointed out that activation processes are already present near the onset temperature T_{onset}[20,34]. Furthermore, it has been observed that, close to T_d, the structural relaxation displays chain-like or fractal structures in colloids[35], which could be related to complex relaxation mechanisms such as dynamic facilitation, and this is supposed to dominate in this regime as

relaxation events in a certain location can induce further relaxation in neighboring sites[36]. As a result, the activation of the CRR may not be the dominant structural relaxation mechanism, and it should not be taken for granted that the two free exponents obtained in an experimental system coincide with the prediction of RFOT, when the effective temperature is relatively high, as our tapped granular systems. Surprisingly, in spite of the possibly mixed relaxation dynamics, the (generalized) AG relation still holds.

In conclusion, we systematically investigate granular packing systems under tap and use the Edwards volume ensemble framework to calculate statistical mechanical quantities. In granular systems, the thermodynamic quantities calculated using the Edwards ensemble are inherently configuration-dependent, satisfying the hypothesis underlying the AG relationship. Furthermore, since the energy barrier is significantly larger than thermal fluctuations in the temperature range of the supercooled granular packings, we consider the effective temperature to be more appropriate for describing the system's state. Upon rescaling the Edwards configurational entropy, we observe a general recovery of the AG relationship. This implies that the relaxation time is predominantly governed by the configurational entropy of the ideal frictionless hard sphere liquid, and that granular materials exhibit properties highly similar to those of glassy systems in both dynamics and statistical mechanics.

The universal relaxation processes in granular systems, along with their strong analogy to hard sphere glass systems, imply that granular materials and hard sphere systems share the same thermodynamic and dynamical properties[5,37,38]. The significance of granular materials as macroscopic models of glassy systems is profound, which can be used to investigate the complex relaxation process in real space close to the dynamical transition temperature.

Methods

We utilize X-ray tomography to reconstruct the three-dimensional structures of granular packings monodisperse spherical particles, the imaging resolution is 0.2 mm (i.e., $D/30$) per pixel. Random packing structures are prepared systematically via mechanical tap. Each tap is driven by a pulse wave generated by an arbitrary waveform generator (Tek AFG3100). Each tap cycle consists of a 1/30 s pulse followed by a 1.5 s interval allowing the system to settle. We employ four types of beads: 3D-printed particles fabricated with a 3D printer with a printing accuracy of 0.032 mm (denoted as 3DP), two kinds of acrylonitrile-butadiene-styrene copolymer particles (denoted as ABS1 and ABS2), and BUMP particles with 150 semi-spheres of diameter $0.1D$ decorated on the sphere surface. The first three types of beads have a diameter of 6 mm, and the BUMP has an outer diameter of 5.8 mm. In addition, the effective friction coefficients decrease in the order of BUMP, 3DP, ABS2, and ABS1. To avoid crystallization, we decorate the internal walls of the container with 5 mm and 8 mm diameter ABS semi-spheres at random positions. Depending on tap intensity Γ, the number of taps needed to reach the stationary states ranges from 10 to 6000. Through image analysis[39,40], we are able to obtain the position and radius of each particle, and calculate all structural parameters of packings. By performing Voronoi tessellation on the packing structure, we calculate the global packing fraction, which is defined as $\phi = \sum V_p / \sum V_{voro}$, where V_{voro} is the volume of Voronoi cells and V_p is the volume of the particle. We set V_p to unity for convenience.

Data availability

All data that support the plots within this paper are available from the corresponding authors on reasonable request.

Received: 4 September 2024; Accepted: 26 March 2025;
Published online: 14 April 2025

References

1. de Gennes, P. G. Granular matter: a tentative view. *Rev. Mod. Phys.* **71**, S374–S382 (1999).
2. Bernal, J. D. A geometrical approach to the structure of liquids. *Nature* **183**, 141–147 (1959).
3. Scott, G. D. Radial distribution of the random close packing of equal spheres. *Nature* **194**, 956–957 (1962).
4. Wang, Y. Granular packing as model glass formers. *Chinese Phys. B* **26**, 14503–014503 (2017).
5. Dauchot, O., Marty, G. & Biroli, G. Dynamical heterogeneity close to the jamming transition in a sheared granular material. *Phys. Rev. Lett.* **95**, 265701 (2005).
6. Yuan, H., Zhang, Z., Kob, W. & Wang, Y. Connecting packing efficiency of binary hard sphere systems to their intermediate range structure. *Phys. Rev. Lett.* **127**, 278001 (2021).
7. Rahmani, Y. et al. Dynamic heterogeneity in hard and soft sphere colloidal glasses. *Soft Matter* **8**, 4264–4270 (2012).
8. Jaeger, H. M., Nagel, S. R. & Behringer, R. P. Granular solids, liquids, and gases. *Rev. Mod. Phys.* **68**, 1259–1273 (1996).
9. Forterre, Y. & Pouliquen, O. Flows of dense granular media. *Annu. Rev. Fluid Mech.* **40**, 1–24 (2008).
10. Adam, G. & Gibbs, J. H. On the temperature dependence of cooperative relaxation properties in glass-forming liquids. *J. Chem. Phys.* **43**, 139–146 (1965).
11. Magill, J. H. Physical properties of aromatic hydrocarbons. III. A test of the Adam–Gibbs relaxation model for glass formers based on the heat-capacity data of 1,3,5-tri-α-naphthylbenzene. *J. Chem. Phys.* **47**, 2802–2807 (1967).
12. Mossa, S. et al. Dynamics and configurational entropy in the Lewis-Wahnström model for supercooled orthoterphenyl. *Phys. Rev. E* **65**, 041205 (2002).
13. Saika-Voivod, I., Poole, P. H. & Sciortino, F. Fragile-to-strong transition and polyamorphism in the energy landscape of liquid silica. *Nature* **412**, 514–517 (2001).
14. Richert, R. & Angell, C. A. Dynamics of glass-forming liquids. V. On the link between molecular dynamics and configurational entropy. *J. Chem. Phys.* **108**, 9016–9026 (1998).
15. Cangialosi, D., Alegría, A. & Colmenero, J. Relationship between dynamics and thermodynamics in glass-forming polymers. *Europhys. Lett.* **70**, 614 (2005).
16. Ngai, K. L. Modification of the Adam−Gibbs model of glass transition for consistency with experimental data. *J. Phys. Chem. B* **103**, 5895–5902 (1999).
17. Kirkpatrick, T. R., Thirumalai, D. & Wolynes, P. G. Scaling concepts for the dynamics of viscous liquids near an ideal glassy state. *Phys. Rev. A* **40**, 1045–1054 (1989).
18. Cavagna, A. Supercooled liquids for pedestrians. *Phys. Rep.* **476**, 51–124 (2009).
19. Grigera, T. S., Cavagna, A., Giardina, I. & Parisi, G. Geometric approach to the dynamic glass transition. *Phys. Rev. Lett.* **88**, 055502 (2002).
20. Brumer, Y. & Reichman, D. R. Mean-field theory, mode-coupling theory, and the onset temperature in supercooled liquids. *Phys. Rev. E* **69**, 041202 (2004).
21. Candelier, R., Dauchot, O. & Biroli, G. Building blocks of dynamical heterogeneities in dense granular media. *Phys. Rev. Lett.* **102**, 088001 (2009).
22. Xia, C. et al. The structural origin of the hard-sphere glass transition in granular packing. *Nat. Commun.* **6**, 8409 (2015).
23. Knight, J. B., Fandrich, C. G., Lau, C. N., Jaeger, H. M. & Nagel, S. R. Density relaxation in a vibrated granular material. *Phys. Rev. E* **51**, 3957–3963 (1995).
24. Philippe, P. & Bideau, D. Compaction dynamics of a granular medium under vertical tapping. *Europhys. Lett.* **60**, 677 (2002).
25. Richard, P., Nicodemi, M., Delannay, R., Ribière, P. & Bideau, D. Slow relaxation and compaction of granular systems. *Nat. Mater.* **4**, 121–128 (2005).

26. Yuan, Y. et al. Experimental test of the Edwards volume ensemble for tapped granular packings. *Phys. Rev. Lett.* **127**, 018002 (2021).
27. Zeng, Z. et al. Equivalence of fluctuation-dissipation and Edwards' temperature in cyclically sheared granular systems. *Phys. Rev. Lett.* **129**, 228004 (2022).
28. Briscoe, C., Song, C., Wang, P. & Makse, H. A. Entropy of jammed matter. *Phys. Rev. Lett.* **101**, 188001 (2008).
29. Xing, Y. et al. Origin of the critical state in sheared granular materials. *Nat. Phys.* **20**, 646–652 (2024).
30. Angelani, L. & Foffi, G. Configurational entropy of hard spheres. *J. Phys-Condens. Mat.* **19**, 256207 (2005).
31. Keys, A. S., Abate, A. R., Glotzer, S. C. & Durian, D. J. Measurement of growing dynamical length scales and prediction of the jamming transition in a granular material. *Nat. Phys.* **3**, 260–264 (2007).
32. Tanaka, H., Kawasaki, T., Shintani, H. & Watanabe, K. Critical-like behaviour of glass-forming liquids. *Nat. Mater.* **9**, 324–331 (2010).
33. Capaccioli, S., Ruocco, G. & Zamponi, F. Dynamically correlated regions and configurational entropy in supercooled liquids. *J. Phys. Chem. B* **112**, 10652–10658 (2008).
34. Bhattacharyya, S. M., Bagchi, B. & Wolynes, P. G. Facilitation, complexity growth, mode coupling, and activated dynamics in supercooled liquids. *Proc. Natl. Acad. Sci. USA* **105**, 16077–16082 (2008).
35. Stevenson, J. D., Schmalian, J. & Wolynes, P. G. The shapes of cooperatively rearranging regions in glass-forming liquids. *Nat. Phys.* **2**, 268–274 (2006).
36. Scalliet, C., Guiselin, B. & Berthier, L. Thirty milliseconds in the life of a supercooled liquid. *Phys. Rev. X* **12**, 041028 (2022).
37. Pouliquen, O., Belzons, M. & Nicolas, M. Fluctuating particle motion during shear induced granular compaction. *Phys. Rev. Lett.* **91**, 014301 (2003).
38. Marty, G. & Dauchot, O. Subdiffusion and Cage effect in a sheared granular material. *Phys. Rev. Lett.* **94**, 015701 (2005).
39. Kou, B. et al. Granular materials flow like complex fluids. *Nature* **551**, 360–363 (2017).
40. Cao, Y. et al. Structural and topological nature of plasticity in sheared granular materials. *Nat. Commun.* **9**, 2911 (2018).

Acknowledgements

The work is supported by the National Natural Science Foundation of China (No. 12274292).

Author contributions

Y.W. designed the research. X.A., H.Y., S.Z., Z.Z., H.L., C.X., and Y.W. performed the experiment. X.A., H.Y., S.Z., Z.Z., C.X., and Y.W. analyzed the data and wrote the paper.

Competing interests

The authors declare no competing interests.

Additional information

Correspondence and requests for materials should be addressed to Chengjie Xia or Yujie Wang.

Peer review information *Communications Physics* thanks the anonymous reviewers for their contribution to the peer review of this work.